Bioorganic & Medicinal Chemistry Letters xxx (2015) xxx–xxx

Contents lists available at ScienceDirect

Bioorganic & Medicinal Chemistry Letters

journal homepage: www.elsevier.com/locate/bmcl

Discovery of EBI-907: A highly potent and orally active B-Raf^{V600E} inhibitor for the treatment of melanoma and associated cancers

Biao Lu [a,*], Hu Cao [a], Jingsong Cao [b], Song Huang [a], Qiyue Hu [a], Dong Liu [b], Ru Shen [b], Xiaodong Shen [a], Weikang Tao [a], Hong Wan [a], Dan Wang [a], Yinfa Yan [b], Liuqing Yang [b], Jiayin Zhang [b], Lei Zhang [a], Lianshan Zhang [c], Minsheng Zhang [b]

[a] *Shanghai Hengrui Pharmaceutical Co., Ltd, 279 Wenjing Rd, Minhang Hi-tech Zone, Shanghai 200245, China*
[b] *Eternity Bioscience Inc., 2005 EastPark Blvd, Cranbury, NJ 08512, USA*
[c] *National Engineering and Research Center for Targeted Drugs, Jiangsu Hengrui Medicine Co., Ltd, 7 Kunlun Shan Road, Lianyungang Economic and Technology Development Zone, Jiangsu Province, China*

ARTICLE INFO

Article history:
Received 19 October 2015
Revised 21 December 2015
Accepted 24 December 2015
Available online xxxx

Keywords:
B-Raf^{V600E}
Kinase
Pyrazolo[3,4-*c*]isoquinoline
Scaffold hopping
Cancer

ABSTRACT

A novel series of pyrazolo[3,4-*c*]isoquinoline derivatives was discovered as B-Raf^{V600E} inhibitors through scaffold hopping based on a literature lead PLX4720. Further SAR exploration and optimization led to the discovery of potent B-Raf^{V600E} inhibitors with good oral bioavailability in rats and dogs. One of the compounds **EBI-907** (**13g**) demonstrated excellent in vivo efficacy in B-Raf^{V600E} dependent Colo-205 tumor xenograft models in mouse and is under preclinical studies for the treatment of melanoma and B-Raf^{V600E} associated cancers.

The Ras/Raf/MEK/ERK pathway plays a key role in regulating cell proliferation, differentiation, and growth. The Raf family of serine/threonine kinases comprises A-Raf, B-Raf, and C-Raf. There is a well established biological mechanism that Raf proteins can signal through phosphorylation and activation of a downstream kinase, mitogen-activated protein MAPK/ERK kinase (MEK), which subsequently phosphorylates and activates extracellular signal-regulated kinase (ERK)[1] that regulates cell proliferation and survival. Mutation in B-Raf drives constitutive activation of the Raf–MEK–ERK pathway which often leads to alteration of gene expression and results in many cancers.[2] The most common B-Raf mutation is a glutamate instead of a valine substitution at position 600 (V600E). So far the oncogenic mutation of B-Raf^{V600E} has been found in 7% of all human cancers, including more than 60% of melanoma, 45% of papillary thyroid cancer, 10% of colorectal cancers, and a small subset of ovarian, breast, lung cancers, and leukemia.[2] Based on its association with human malignancies, B-Raf has been a target of high interest to treat cancer in recent decades.[3] Herein, we report our discovery of a highly potent and orally efficacious B-Raf^{V600E} inhibitor **EBI-907** (**13g**) with a novel biaryl scaffold featured pyrazolo[3,4-*c*]isoquinoline.

There are many Braf-specific inhibitors with different scaffolds reported in the literature. Vemurafenib (PLX4032)[4] with an aza-indole core was developed by Plexxikon and Roche and became the first marketed drug for treatments of patients with unresectable and metastatic melanoma. Dabrafenib (GSK2118436)[5] with a pyrimidine substituted thiazole core was later approved as well by FDA. It is noteworthy that the analogue PLX4720 showed similar activity in vitro and in vivo as Vemurafenib. The latter was selected over PLX4720 because it has more scalable pharmacokinetic properties.[6] Besides, there are other chemotypes of B-Raf^{V600E} inhibitors at different clinical stages including BGB283 (BeiGene),[7] LGX818 (Novartis),[8] LY3009120 (Lilly),[9] MLN2480[10] (Takeda) and others in preclinical development[11] (Fig. 1).

On the basis of the co-crystal structures of Vemurafenib and its analog PLX4720 published (pdb codes 3C4C, Fig. 2),[12] we were able to identify the key binding interactions of PLX4720 to an 'active' conformation unique to the RAF proteins, in which the DFG motif is in the 'DFG-in' conformation but the αC helix is moved outward from the active site by the lipophilic alkyl group. The sulfonamide moiety is engaged in very important interactions with key residues such as Asp-594 and Phe-595, Lys-483 via hydrogen bonds.[12] The N and NH of the aza-indole core are making interactions with the hinge residues Thr-529, Gln-530, and Trp-531. By breaking

* Corresponding author.

http://dx.doi.org/10.1016/j.bmcl.2015.12.086
0960-894X/

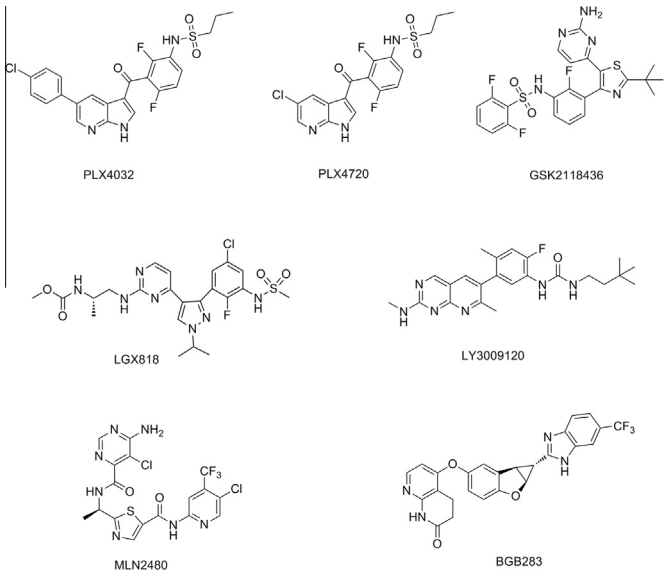

Figure 1. Structures of representative B-Raf^{V600E} inhibitors.

the indole 5-membered ring and building a new fused ring from the carbonyl position, we envisioned a novel scaffold of 3-aminoisoquinoline which will make the same hinge interaction with Trp-531 and pick up new interactions with Cys-532 (Fig. 2) from which a new series of B-Raf^{V600E} inhibitors could be developed.[13]

To test this idea, we rapidly synthesized compound **1** as shown in Scheme 1. 3-Bromo-benzonitrile **2** was reduced by using BH_3·THF to its benzylic amine **3**, which was condensed with acetimidate to afford acetimidamide intermediate **4**. The subsequent ring closure reaction was carried out in *conc*d sulfuric acid to give the isoquinoline core **5**,[14] which was converted to the boronic ester **6** via Miyaura reaction. The boronic ester was coupled with aryl bromide piece via Suzuki reaction to give the target product **1**.

Compound **1** showed 8.7 μM potency in biochemical assays performed using LanthaScreen™. It was 39 times weaker than PLX4720 (220 nM). The micromolar enzymatic activity revealed that additional interactions would be necessary to achieve enough potency. The carbonyl oxygen of PLX4720 could accept an H-bond

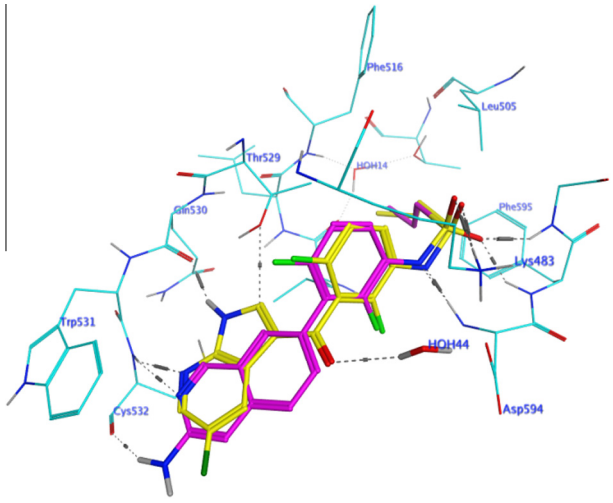

Figure 2. Our initial design. Crystal structure conformation of PLX4720 (yellow) and modeled binding conformation of **1** (cyan) within the crystal structure conformation of B-Raf protein from pdb:3C4C.

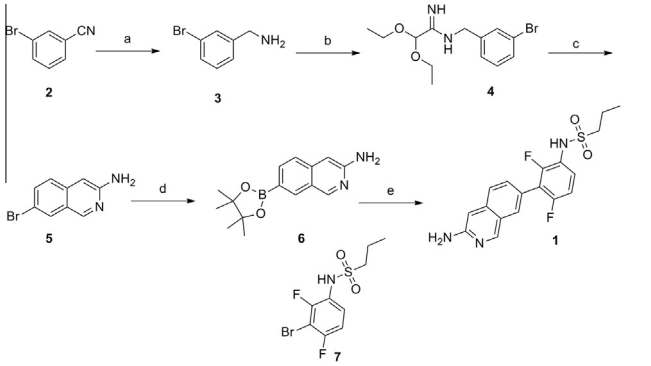

Scheme 1. Synthesis of compound **1**. Reagents and conditions: (a) BH_3·THF, THF, reflux; (b) methyl 2,2-diethoxyacetimidate, 70 °C; (c) concd H_2SO_4, 40 °C; (d) bis (pinacolato)diboron, $Pd(dppf)Cl_2$, KOAc, dioxane 120 °C; (e) **7**, $Pd(dppf)Cl_2$, Na_2CO_3, wet DME, 120 °C, microwave.

from a crystallographic water molecule (HOH44), as shown in Figure 2 and increase potency based on Plexxikon's pivotal work.[12] We thought that hydrogen bonding acceptor capability of the carbonyl group may be mimicked by an oxygen-bearing group such as a methoxyl at the 6-position on the isoquinoline ring. On the other hand, the amine group of compound **1** may be substituted by employing LGX818's side chain to enhance potency as well.[15] Consequently, we started from different 4-substituted 3-bromo-benzonitrile to synthesize corresponding analogs **8a** and **8b** by similar route. Meanwhile, compound **1** and compounds **8a**/**8b** were reacted with methyl *N*-(1-oxopropan-2-yl) carbamate via reductive amination to obtain *N*-substituted analogs of compounds **9**–**12** (Scheme 2).

A summary of SAR for the isoquinoline series is shown in Table 1. Compound **10** bearing LGX-818's side chain was 10 times more potent than compound **1** in biochemical assay although its cellular activity was not potent enough. However, compound **9** with the wrong configuration tail showed no activity at all. Fortunately, 6-methoxyl substituted isoquinoline analog **8a** exhibited 10 times more potent enzymatic activity and 1.2 μM cellular potency. Next, we examined compound **11** with both 6-substituted methoxyl and LGX-818's side chain. Its enzymatic activity and cellular activity were dramatically improved to 100 nM and 20 nM, respectively. To understand the role of methoxyl group, we synthesized ethyl substituted analog **12**, which was 6 times less potent than

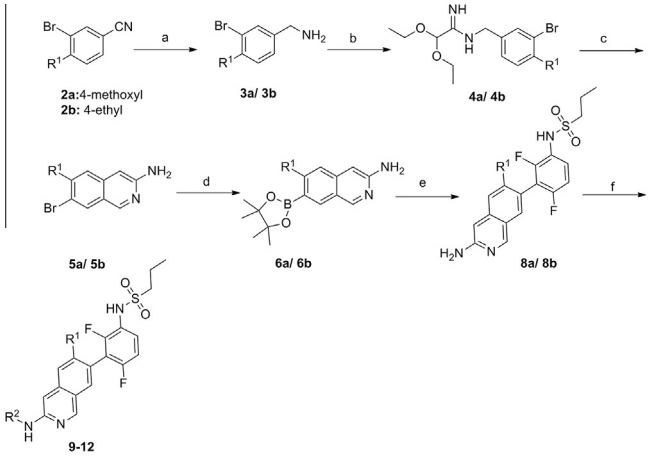

Scheme 2. Synthesis of analogs of compound **1**. Reagents and conditions: (a) BH_3·THF, THF, reflux; (b) methyl 2,2-diethoxyacetimidate, 70 °C, (c) concd H_2SO_4, 40 °C; (d) bis-(pinacolato)diboron, $Pd(dppf)Cl_2$, KOAc, dioxane, 120 °C; (e) **7**, $Pd(dppf)Cl_2$, K_2CO_3, wet DMF, 120 °C; (f) R^2-aldehyde, $NaBH_3CN$, HOAc, MeOH.

Table 1
Selected SAR of isoquinoline series

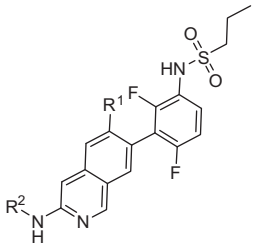

Compd	R^1	R^2	$Braf^{V600E}$ Lantha[a] IC_{50} (μM)	A375 cell growth[a] IC_{50} (μM)
1	H	H	8.7	n.d[b]
9	H	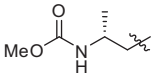	>30	n.d
10	H	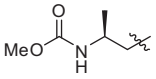	0.8	2.7
8a	MeO	H	0.8	1.2
11	MeO	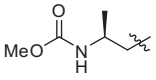	0.1	0.02
12	Et	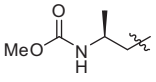	0.6	0.3

[a] Data represent mean value of at least two experiments.
[b] n.d. = not determined.

compound **11**. These results further supported our hypothesis that the methoxyl group at the 6-position of isoquinoline ring may indeed increase the binding affinity via polar or H-bond interactions.

Although compound **11** was potent enough for in vivo study, we were concerned about its carbamate fragment for potential metabolic instability. At that time Wenglowsky et al. published a set of B-Raf inhibitors.[11c] One of them, compound **17**, was co-crystalized with B-Raf (pdb:3TV6). Based on the 3D alignment of their compound and the modeled pose of our compound **11** in the crystal structure (Fig. 3), the pyrazole ring is in a good position to fuse with our isoquinoline core. It seems that it will not only lock in the NH hydrogen bonding interaction with Cys-532, but also form a π–π stacking interaction with Trp-531. We ventured to replace the carbamate side chain with pyrazolo[3,4-*c*]isoquinoline core by fusing another 5 membered ring onto the isoquinoline analog **11** (Fig. 3).

The synthetic approach for the preparation of pyrazolo[3,4-*c*] isoquinoline analogs is outlined in Scheme 3. 4-Bromo-3-methoxyl benzoic acid **14** was reduced to its benzylic alcohol, followed by bromination and cyanation to afford benzylic nitrile intermediate **17**. After treatment with sodium hydride (or LiHMDS), it was condensed with methyl formic ester (or acyl chloride) smoothly to give functionalized nitrile **18a**–**b** which was condensed with benzyl hydrazine to form benzylic pyrozole intermediate **19a**–**b**.[16] The following assembly of its isoquinoline ring underwent through Pictet–Spengler type reaction.[17] The obtained bromo piece was converted to its boronic ester which was further coupled with another bromo fragment **22** to give biaryl intermediate **23a**–**h** via Suzuki reaction. Subsequent debenzylation reaction turned out to be difficult. Initial attempts using hydrogenation (Pd/C, H_2) or KO^{t}Bu/DMSO with O_2 was not successful.[17] Finally, upon heating **23a**–**h** in formic acid via palladium mediated transfer hydrogenation gave analogs **13a**–**h** in modest yields.[18]

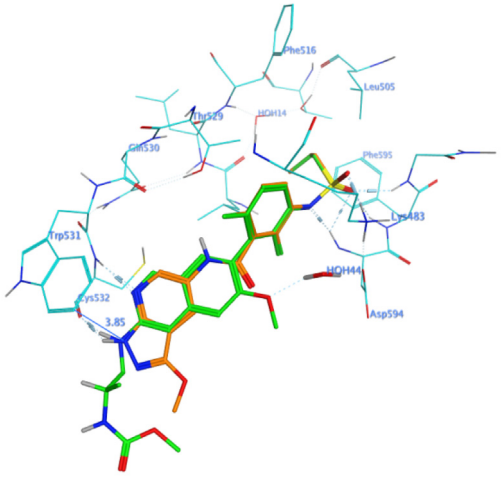

Crystal structure conformation of Wenglowsky's compound 17 from pdb:3TV6 (Orange) and modeled binding conformation of **11** (Green) within the crystal structure conformation of B-Raf protein from pdb:3OG7.

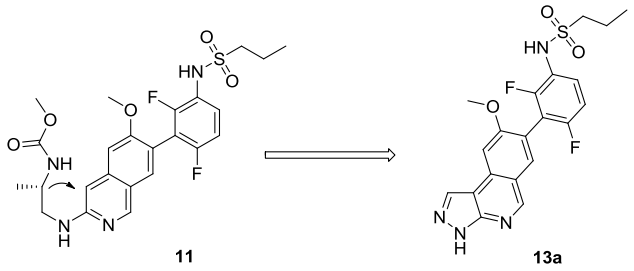

Figure 3. Our modified design.

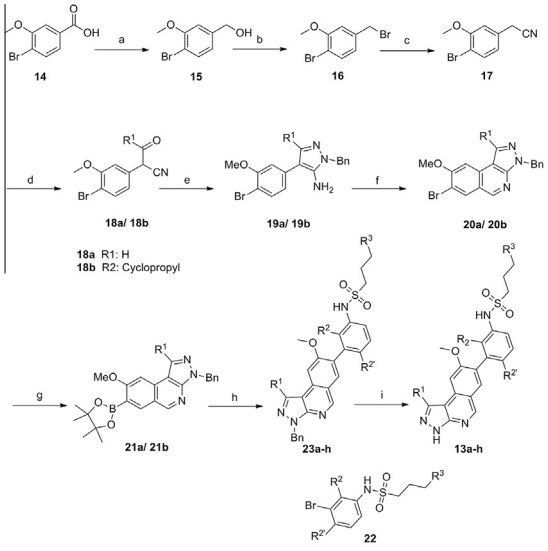

Scheme 3. Synthesis of analogs **13**. Reactions and conditions: (a) BH_3, THF; (b) BBr_3, Et_2O; (c) KCN/18-crown-6, DMEO; (d) melhyl formate or cydopropanecarbonyl chloride, NaH or LiHMDSJHF; (e) benzyl hydrazine, HOAc, ^{i}PrOH, 70 °C; (f) $(HCHO)_n$, TFA, reilux; (g) bis (pinacolato)diboron, $Pd(dppf)_2Cl_2$, KOAc, dioxane, 110 °C; (h) **22**, $Pd(dppf)_2Cl_2$, K_3PO_4, dioxane, 110 °C; (i) 2W 20% $Pd(OH)_2$, ammonium formic, fomic acid, 100 °C.

As expected, pyrazolo[3,4-*c*]isoquinoline analogs also showed potent inhibition in both LanthaScreen™ and A375 cell proliferation assays. Their SAR is summarized in Table 2. Compound **13a**

Table 2
Selected SAR of pyrazolo[3,4-*c*]isoquinoline series

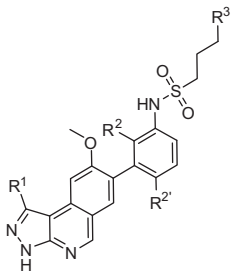

Compd	R^1	$R^2/R^{2'}$	R^3	$Braf^{V600E}$ Lantha[a] IC_{50} (nM)	A375 cell growth[a] IC_{50} (nM)
13a	H	F/F	H	70	138
13b	H	Cl/F	H	11	47
13c	H	Cl/Cl	H	20	340
13d	H	Cl/F	F	7	220
13e		F/F	H	220	135
13f		Cl/F	H	80	313
13g		Cl/F	F	7	13
13h		Cl/F	CH_3	17	435

[a] Data represent mean value of at least two experiments.

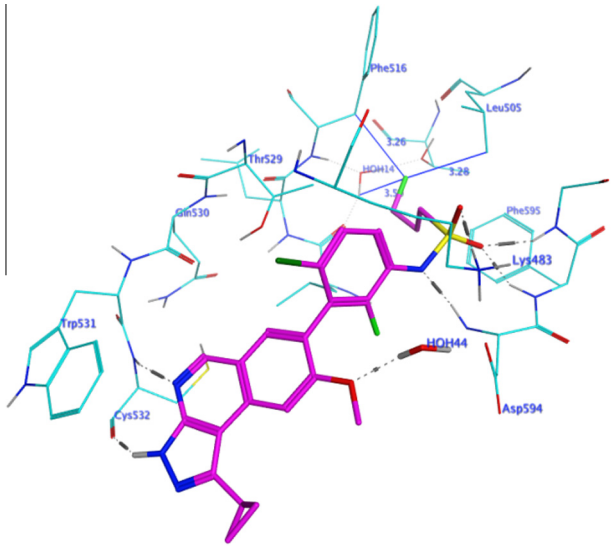

Figure 4. The binding pose of **13g** to B-Raf protein.

gave comparable enzyme activity to aminoisoquinoline analog **11**. When changing one of fluorine to chlorine on the right benzene ring of **13a**, enzymatic activity of **13b** was dramatically improved by 5 times although cellular activity was dropped a little. However,

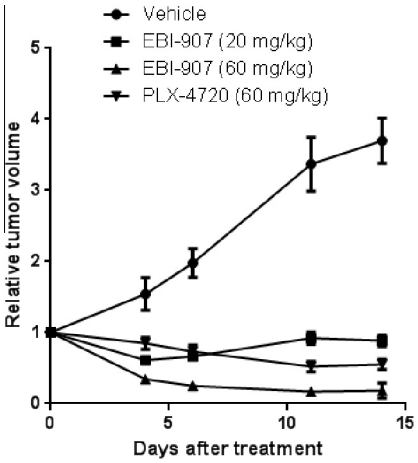

Figure 5. Colo-205 xenograft mice model.

dichloro substituted analog **13c** was less potent than **13b**. By putting one fluorine atom into the side chain of **13b**, enzymatic activity of compound **13d** reached single digit nanomolar (7 nM), but its cellular activity was lowered. To fix this issue and eliminate potential metabolic soft spot, we assembled a cyclopropyl onto 3-position of the pyrazole.[19] Compounds **13e**, **13f** and **13h** were less potent as well, but compound **13g** demonstrated excellent A375 cellular activity with IC_{50} 13 nM. In the other cell line Colo-205, it also showed good potency with IC_{50} of 14 nM. In contrast, **13g** did not show meaningful anti-proliferative effects on the growth of Calu-6 cells carrying a wild-type B-Raf, exhibiting at least 40-fold (455 nM) selectivity towards $B\text{-}Raf^{V600E}$-dependent cells lines. The modeled binding pose of **13g** is shown in Figure 4. In addition to the same key hinge interactions and backpocket sulfonamide interactions as **1**, **13g** also forms the same key hydrogen bond interaction with HOH44 as PLX4720. The terminal Fluoro group is placed in close Van der Waals contacts with Phe-516, Leu-505 and tightly bound crystal water HOH14 as well.

Furthermore, compound **13g** exhibited excellent liver microsomal stability in different species ($T_{1/2}$ Human/Rat/Mouse: 350/148/81 min). Based on the above data, **13g** became our candidate for in vivo study.[20] It displayed desired in vivo pharmacokinetics as shown in Table 3. After a single 5 mg/kg oral dose of a solution of **13g** to rats, its AUC_{0-24} reached 14186 ng/ml * h. **13g** also showed AUC_{0-24} of 8906 ng/ml * h in dogs with a single 2 mg/kg oral dose. Its oral bioavailability for rats and dogs was 20% and 40%, respectively.

The efficacy of **13g** in vivo was evaluated in a $B\text{-}Raf^{V600E}$-dependent human Colo-205 tumor xenograft mouse model as shown in Figure 5. Compound **13g** was administered orally at 20 mg/kg and 60 mg/kg daily in a 14 days (QD) with the reference compound PLX4720 60 mg/kg as a positive control. PLX4720 showed 85% tumor growth inhibition. Compound **13g** caused a partial (76%,

Table 3
The PK parameters of **13g** (**EBI-907**) in rats and dogs

Species/route/dose	C_{max} (ng/ml)	$AUC_{0.24}$ (ng/ml * h)	$T_{1,2}$ (h)	Cl (ml/min/kg)	V_{ss} (L/kg)	*F* (%)
Rat/iv[a]/0.5 mg/kg		7224	3.4	1.2	0.34	
Rat/po[b]/5 mg/kg	1498	14,186				20
Dog/iv/0.2 mg/kg		2201	7.8	1.4	0.91	
Dog/po/2 mg/kg	972	8906				40

[a] iv: intravenous injection.
[b] po: oral administration.

20 mg/kg) or complete tumor regression (95%, 60 mg/kg) in a dose-dependent manner, with superior efficacy over PLX4720 ($P = 0.012$). It was noteworthy that no significant changes in body weights of all treatment groups were observed.

In summary, we developed a novel class of B-Raf^{V600E} inhibitor with biaryl structure featured pyrazolo[3,4-*c*]isoquinoline core via two consecutive scaffold hopping from the literature lead PLX4720. One of the optimized analogs **EBI-907** (**13g**) demonstrated both excellent potency in vitro and superior efficacy in vivo. Further development studies of this molecule are in progress and more detailed results will be disclosed in due course.

Acknowledgements

We thank members of the analytical group of Shanghai Hengrui Pharmaceutical Ltd for their analytical and spectral determinations, and the Informatics group as well as Drs. Hejun Lv and Jun Feng for their useful discussions and enormous support.

References and notes

1. (a) Peyssonnaux, C.; Eychene, A. *Biol. Cell* **2001**, *93*, 53; (b) McCubrey, J. A.; Milella, M.; Tafuri, A.; Martelli, A. M.; Lunghi, P.; Bonati, A.; Cervello, M.; Lee, J. T.; Steelman, L. S. *Curr. Opin. Investig. Drugs* **2008**, *9*, 614.
2. (a) Davies, H.; Bignell, G. R.; Cox, C.; Stephens, P.; Edkins, S.; Clegg, S.; Teague, J.; Woffendin, H.; Garnett, M. J.; Bottomley, W.; Davis, N.; Dicks, E.; Ewing, R.; Floyd, Y.; Gray, K.; Hall, S.; Hawes, R.; Hughes, J.; Kosmidou, V.; Menzies, A.; Mould, C.; Parker, A.; Stevens, C.; Watt, S.; Hooper, S.; Wilson, R.; Jayatilake, H.; Guster-son, B. A.; Cooper, C.; Shipley, J.; Hargrave, D.; Pritchard-Jones, K.; Maitland, N.; Chenevix-Trench, G.; Riggins, G. J.; Bigner, D. D.; Palmieri, G.; Cossu, A.; Flanagan, A.; Nicholson, A.; Ho, J. W. C.; Leung, S. Y.; Yuen, S. T.; Weber, B. L.; Seigler, H. F.; Darrow, T. L.; Paterson, H.; Marais, R.; Marshall, C. J.; Wooster, R.; Stratton, M. R.; Futreal, P. A. *Nature* **2002**, *417*, 949; (b) Michaloglou, C.; Vredeveld, L. C.; Mooi, W. J.; Peeper, D. S. *Oncogene* **2008**, *27*, 877.
3. (a) Huang, T.; Karsy, M.; Zhuge, J.; Zhong, M.; Liu, D. *J. Hematol. Oncol.* **2013**, *6*, 30; (b) Zambon, A.; Niculescu-Duvaz, I.; Niculescu-Duvaz, D.; Marais, R.; Springer, C. J. *Bioorg. Med. Chem. Lett.* **2012**, *22*, 789.
4. Smalley, K. S. M. *Curr. Opin. Investig. Drugs* **2010**, *11*, 699.
5. Rheault, T. R.; Stellwagen, J. C.; Adjabeng, G. M.; Hornberger, K. R.; Petrov, K. G.; Waterson, A. G.; Dickerson, S. H.; Mook, R. A.; Laquerre, S. G.; King, A. J.; Rossanese, O. W.; Arnone, M. R.; Smitheman, K. N.; Kane-Carson, L. S.; Han, C.; Moorthy, G. S.; Moss, K. G.; Uehling, D. E. *ACS Med. Chem. Lett.* **2013**, *4*, 358.
6. Bollag, G.; Hirth, P.; Tsai, J.; Zhang, J.; Ibrahim, P. N.; Cho, H.; Spevak, W.; Zhang, C.; Zhang, Y.; Habets, G.; Burton, E. A.; Wong, B.; Tsang, G.; West, B. L.; Powell, B.; Shellooe, R.; Marimuthu, A.; Nguyen, H.; Zhang, K. Y. J.; Artis, D. R.; Schlessinger, J.; Su, F.; Higgins, B.; Iyer, R.; D'Andrea, K.; Koehler, A.; Stumm, M.; Lin, P. S.; Lee, R. J.; Grippo, J.; Puzanov, I.; Kim, K. B.; Ribas, A.; McAr-thur, G. A.; Sosman, J. A.; Chapman, P. B.; Flaherty, K. T.; Xu, X.; Nathanson, K. L.; Nolop, K. *Nature* **2010**, *467*, 596.
7. Tang, Z.; Hu, X.; Gong, W.; Liu, Y.; Gao, Y.; Sutton, D.; Wang, L.; Yuan, X.; Du, R.; Cheung, S.-H.; Wei, J.; Zhao, Y.; Luo, L.; Zhang, G.; Wang, S.; Zhou, C.; Feng, Y.; Peng, H.; Zhang, Y.; Du, Y.; Liu, Y.; Li, S.; Hao, R.; Wei, M.; Ji, J.-F.; Zhang, L.-H.; Li, S. *Mol. Cancer Ther.* **2015**, *14*, 2187.
8. Anforth, R. M.; Carlos, G. R. M.; Scolyer, R. A.; Chou, S.; Fer-nandez-Penas, P. *Melanoma Res.* **2015**, *25*, 91.
9. Henry, J. R.; Kaufman, M. D.; Peng, S.; Ahn, Y. M.; Caldwell, T. M.; Vogeti, L.; Telikepalli, H.; Lu, W.; Hood, M. M.; Rutkoski, T. J.; Smith, B. D.; Vogeti, S.; Miller, D.; Wise, S. C.; Chun, L.; Zhang, X.; Zhang, Y.; Kays, L.; Hipskind, P. A.; Wrobleski, A. D.; Lobb, K. L.; Clay, J. M.; Cohen, J. D.; Walgren, J. L.; McCann, D.; Patel, P.; Clawson, D. K.; Guo, S.; Manglicmot, D.; Groshong, C.; Logan, C.; Starling, J. J.; Flynn, D. L. *J. Med. Chem.* **2015**, *58*, 4165.
10. Stewart, M. L.; Tamayo, P.; Wilson, A. J.; Wang, S.; Chang, Y. M.; Kim, J. W.; Khabele, D.; Shamji, A. F.; Schreiber, S. L. *Cancer Res.* **2015**, *75*, 2897.
11. (a) Pulici, M.; Traquandi, G.; Marchionni, C.; Modugno, M.; Lupi, R.; Amboldi, N.; Casale, E.; Colombo, N.; Corti, L.; Fasolini, M.; Gasparri, F.; Pastori, W.; Scolaro, A.; Donati, D.; Felder, E.; Galvani, A.; Isacchi, A.; Pesenti, E.; Ciomei, M. *ChemMedChem* **2015**, *10*, 276; (b) Cheng, H.; Chang, Y.; Zhang, L.; Luo, J.; Tu, Z.; Lu, X.; Zhang, Q.; Lu, J.; Ren, X.; Ding, K. *J. Med. Chem.* **2014**, *57*, 2692; (c) Wenglowsky, S.; Ren, L.; Ahrendt, K. A.; Laird, E. R.; Aliagas, I.; Alicke, B.; Buckmelter, A. J.; Choo, E. F.; Dinkel, V.; Feng, B.; Gloor, S. L.; Gould, S. E.; Gross, S.; Gunzner-Toste, J.; Hansen, J. D.; Hatzivassiliou, G.; Liu, B.; Malesky, K.; Mathieu, S.; Newhouse, B.; Raddatz, N. J.; Ran, Y.; Rana, S.; Randolph, N.; Risom, T.; Rudolph, J.; Savage, S.; Selby, L. T.; Shrag, M.; Song, K.; Sturgis, H. L.; Voegtli, W. C.; Wen, Z.; Willis, B. S.; Woessner, R. D.; Wu, W.; Young, W. B.; Grina, J. *ACS Med. Chem. Lett.* **2011**, *2*, 342.
12. Tsai, J.; Lee, J. T.; Wang, W.; Zhang, J.; Cho, H.; Mamo, S.; Bremer, R.; Gillette, S.; Kong, J.; Haass, N. K.; Sproesser, K.; Li, L.; Smalley, K. S.; Fong, D.; Zhu, Y. L.; Marimuthu, A.; Nguyen, H.; Lam, B.; Liu, J.; Cheung, I.; Rice, J.; Suzuki, Y.; Luu, C.; Settachat-gul, C.; Shellooe, R.; Cantwell, J.; Kim, S. H.; Schlessinger, J.; Zhang, K. Y.; West, B. L.; Powell, B.; Habets, G.; Zhang, C.; Ibrahim, P. N.; Hirth, P.; Artis, D. R.; Herlyn, M.; Bollag, G. *Proc. Natl. Acad. Sci. U.S.A.* **2008**, *105*, 3041.
13. Ren reported a class of B-Raf^{V600E} inhibitor with pyridopyrimidin-7-one scaffold similar as our initial design during the time when we worked on B-Raf project. One of analogs was exactly our lead compound **1**, showing weak potency. See: Ren, L.; Ahrendt, K. A.; Grina, J.; Laird, E. R.; Buckmelter, A. J.; Hansen, J. D.; Newhouse, B.; Moreno, D.; Wenglowsky, S.; Dinkel, V.; Gloor, S. L.; Hastings, G.; Rana, S.; Rasor, K.; Risom, T.; Sturgis, H. L.; Voegtli, W. C.; Mathieu, S. *Bioorg. Med. Chem. Lett.* **2012**, *22*, 3387.
14. Huang, L.; Liu, S.; Lunney, E.; Planken, WO2007125405.
15. Some SAR information about LGX813 was shown in one of Novartis patents (see: Huang, S.; Jin, X.; Liu, Z.; Poon, D.; Tellew, J.; Wan, Y.; Wang, X.; Xie, Y. WO 2011025927).
16. Bogza, S. L.; Ivanov, A. V.; Dulenko, V. I.; Kobrakov, K. I. *Chem. Heterocycl. Compd. (New York, NY, United States)* **1997**, *33*, 69.
17. Bogza, S. L.; Kobrakov, K. I.; Malienko, A. A.; Sujkov, S. Y.; Perepichka, I. F.; Bryce, M. R.; Bogdan, N. M.; Dulenko, V. I. *J. Heterocycl. Chem.* **2001**, *38*, 523.
18. Haddach, A. A.; Kelleman, A.; Deaton-Rewolinskia, M. V. *Tetrahedron Lett.* **2002**, *43*, 399.
19. Wenglowsky, S.; Moreno, D.; Rudolph, J.; Ran, Y.; Ahrendt, K. A.; Arrigo, A.; Colson, B.; Gloor, S. L.; Gregg Hastings, G. *Bioorg. Med. Chem. Lett.* **2012**, *22*, 912.
20. All new compounds are fully characterized. Data for compound **13g**: ^{1}H NMR (400 MHz, DMSO-d_6) δ: 9.73 (s, 1H), 9.03 (s, 1H), 8.14 (s, 1H), 8.03 (s, 1H), 7.58 (dd, J = 8.8, 6.0 Hz, 1H), 7.40 (dd, J = 8.8, 8.4 Hz, 1H), 4.57 (dt, J = 47.2, 6.0 Hz, 2H), 3.99 (s, 1H), 3.26–3.30 (m, 2H), 2.59 (m, 1H), 2.11–2.23 (m, 2H), 1.10–1.15 (m, 2H), 0.96–1.0 (m, 2H); ^{13}C NMR (100 MHz, DMSO-d_6) δ 159.2, 158.0 (d, J = 244.3 Hz), 152.3, 150.3, 146.0, 133.1, 132.6, 131.4 (d, J = 4.4 Hz), 130.7 (d, J = 3.6 Hz), 129.1 (d, J = 8.8 Hz), 125.5 (d, J = 21 Hz), 120.4, 119.2, 114.6 (d, J = 23.8 Hz), 106.3, 101.9, 81.9 (d, J = 161.9 Hz), 56.0, 49.2 (d, J = 5.1 Hz), 24.7 (d, J = 20.4 Hz), 9.3, 6.3, 6.2; LC–MS: 507 (M+1). HRMS (EI+) m/z: Calcd $C_{23}H_{21}ClF_2N_4O_3S$ (M+1) 507.1069, found 507.1046 (M+1).